

1 Network Architecture and Mutational Sensitivity of the *C. elegans* Metabolome

2

3 Lindsay M. Johnson<sup>1,†</sup>, Luke M. Chandler<sup>2,†</sup>, Sarah K. Davies<sup>3</sup> and Charles F. Baer<sup>1,2,\*</sup>

4

5 1 – Department of Biology, University of Florida, Gainesville, FL

6 2 – University of Florida Genetics Institute

7 3 - Faculty of Medicine, Department of Surgery & Cancer, Imperial College, London

8 † - these authors contributed equally

9

10 Email: [lindsaymjohnson@ufl.edu](mailto:lindsaymjohnson@ufl.edu); [lukemchandler@ufl.edu](mailto:lukemchandler@ufl.edu); [sarah.davies1@imperial.ed.ac.uk](mailto:sarah.davies1@imperial.ed.ac.uk)

11 \* Correspondence to:

12 Charles F. Baer

13 Department of Biology

14 University of Florida

15 P. O. Box 118525

16 Gainesville, FL 32611-8525 USA

17 Email: [cbaer@ufl.edu](mailto:cbaer@ufl.edu)

18

19 Keywords: metabolic network, mutation accumulation, mutational correlation, mutational

20 variance, network centrality

21

22 **Declarations:**

- 23 ○ Ethics approval and consent to participate: Not applicable
- 24 ○ Consent for publication: Not applicable
- 25 ○ Availability of data and material:
- 26 ○ Metabolomics data (normalized metabolite concentrations) are archived in Dryad
- 27 (<http://dx.doi.org/10.5061/dryad.2dn09/1>).
- 28 ○ Data used to reconstruct the metabolic networks are included in Supplementary
- 29 Appendix A1.
- 30 ○ Competing interests: The authors declare no competing interests.
- 31 ○ Funding: Funding was provided by NIH grant R01GM107227 to CFB and E. C. Andersen.
- 32 The funding agency had no role in the design of the study and the collection, analysis, and
- 33 interpretation of the data or in the writing of the manuscript.
- 34 ○ Authors' contributions. LMJ and LMC collected and analyzed data in the network
- 35 reconstruction and contributed to writing the manuscript. SKD collected and analyzed the
- 36 GC-MS data. CFB analyzed data and wrote the manuscript. All authors read and approved
- 37 the final manuscript.
- 38 ○ Acknowledgements: This work was initially conceived by Armand Leroi and Jake Bundy.
- 39 We thank Art Edison, Dan Hahn, Tom Hladish, Marta Wayne, Michael Witting, and several
- 40 anonymous reviewers for their generosity and helpful advice. We especially thank Hongwu
- 41 Ma for leading us to and through his metabolite database and Reviewer #3 for his/her many
- 42 insightful comments and suggestions. Support was provided by NIH grant R01GM107227 to
- 43 CFB and E. C. Andersen.

44

45 List of Figures and Tables

46 **Figure 1.** (a) Design of an MA experiment (b) Fitness, Trait means vs.  $gen(MA)$  and  $VG$  vs.

47  $gen(MA)$  (c)  $Cov(G)$  vs.  $gen(MA)$

48 **Figure 2.** Metabolic Network

49 **Figure 3.** Depiction of  $k$ -core

50 **Figure 4.** Plot of first canonical variates of mutation parameters (Y-axis) vs. network parameters

51 (X-axis).

52 **Figure 5.** Parametric bootstrap distributions of random correlations between (a)  $r_M$  and shortest

53 path length in the directed network, (b)  $|r_M|$  and shortest directed path length, (c)  $r_M$  and shortest

54 path length in the undirected network (i.e., shorter of the two path lengths between metabolites  $i$

55 and  $j$  in the directed network).

56

57 **Table 1.** List of definitions of network statistics and mutational parameters

58 **Table 2.** Correlations between network statistics and mutational parameters

59

60 **Supplementary Figure S1.** Depiction of shortest path length in a directed network.

61 **Supplementary Figure S2.** Plots of mutational parameters vs. network statistics.

62 **Supplementary Figure S3.** Bootstrap distributions of  $r_M$  with six randomly chosen covariates.

63

64 **Supplementary Table S1.** Network and mutational parameters of metabolites. (Excel)

65 **Supplementary Table S2.** Table of discrepancies between MZ and YW methods (Word)

66 **Supplementary Table S3.** Canonical correlation analysis (Word).

67 **Supplementary Table S4.** Mutational and environmental correlations (Excel)

- 68 **Supplementary Table S5.** Shortest network path lengths (Excel)
- 69 **Supplementary Data Set 1.** Metabolic network data (Excel)

In review

70 **Abstract**

71 A fundamental issue in evolutionary systems biology is understanding the relationship between  
72 the topological architecture of a biological network, such as a metabolic network, and the  
73 evolution of the network. The rate at which an element in a metabolic network accumulates  
74 genetic variation via new mutations depends on both the size of the mutational target it presents  
75 and its robustness to mutational perturbation. Quantifying the relationship between topological  
76 properties of network elements and the mutability of those elements will facilitate understanding  
77 the variation in and evolution of networks at the level of populations and higher taxa.

78 We report an investigation into the relationship between two topological properties of 29  
79 metabolites in the *C. elegans* metabolic network and the sensitivity of those metabolites to the  
80 cumulative effects of spontaneous mutation. The correlations between measures of network  
81 centrality and mutability are not statistically significant, but several trends point toward a weak  
82 positive association between network centrality and mutational sensitivity. There is a small but  
83 significant negative association between the mutational correlation of a pair of metabolites ( $r_M$ )  
84 and the shortest path length between those metabolites.

85 Positive association between the centrality of a metabolite and its mutational heritability  
86 is consistent with centrally-positioned metabolites presenting a larger mutational target than  
87 peripheral ones, and is inconsistent with centrality conferring mutational robustness, at least *in*  
88 *toto*. The weakness of the correlation between  $r_M$  and the shortest path length between pairs of  
89 metabolites suggests that network locality is an important but not overwhelming factor governing  
90 mutational pleiotropy. These findings provide necessary background against which the effects of  
91 other evolutionary forces, most importantly natural selection, can be interpreted.

92 **Introduction:**

93           The set of chemical reactions that constitute organismal metabolism is often represented  
94 as a network of interacting components, in which individual metabolites are the nodes in the  
95 network and the chemical reactions of metabolism are the edges linking the nodes (Jeong et al.,  
96 2000). Representation of a complex biological process such as metabolism as a network is  
97 conceptually powerful because it offers a convenient and familiar way of visualizing the system,  
98 as well as a well-developed mathematical framework for analysis.

99           If the representation of a biological system as a network is to be useful as more than a  
100 metaphor, it must have predictive power (Winterbach et al., 2013). Metabolic networks have  
101 been investigated in the context of evolution, toward a variety of ends. Many studies have  
102 compared empirical metabolic networks to various random networks, with the goal of inferring  
103 adaptive features of network architecture (e.g., Fell and Wagner, 2000; Jeong et al., 2000; Wagner  
104 and Fell, 2001; Siegal et al., 2007; Minnhagen and Bernhardsson, 2008; Papp et al.,  
105 2009; Bernhardsson and Minnhagen, 2010). Other studies have addressed the relationship  
106 between network-level properties of individual elements of the network (e.g., node degree,  
107 centrality) and properties such as rates of protein evolution (Vitkup et al., 2006; Greenberg et al.,  
108 2008), within-species polymorphism (Hudson and Conant, 2011), and mutational robustness  
109 (Levy and Siegal, 2008).

110           One fundamental evolutionary process that remains essentially unexplored with respect to  
111 metabolic networks is mutation. Mutation is the ultimate source of genetic variation, and as such  
112 provides the raw material for evolution: the greater the input of genetic variation by mutation, the  
113 greater the capacity for evolution. However, in a well-adapted population, most mutations are at  
114 least slightly deleterious. At equilibrium, the standing genetic variation in a population

115 represents a balance between the input of new mutations that increase genetic variation and  
116 reduce fitness, and natural selection, which removes deleterious variants and thereby increases  
117 fitness. Because genetic variation is jointly governed by mutation and selection, understanding  
118 the evolution of any biological entity, such as a metabolic network, requires an independent  
119 accounting of the effects of mutation and selection.

120         The cumulative effects of spontaneous mutations can be assessed in the near absence of  
121 natural selection by means of a mutation accumulation (MA) experiment (Figure 1). Selection  
122 becomes ineffective relative to random genetic drift in small populations, and mutations with  
123 effects on fitness smaller than about the reciprocal of the population size (technically, the genetic  
124 effective population size,  $N_e$ ) will be essentially invisible to natural selection (Kimura, 1968).  
125 An MA experiment minimizes the efficacy of selection by minimizing  $N_e$ , thereby allowing all  
126 but the most strongly deleterious mutations to evolve as if they are invisible to selection  
127 (Halligan and Keightley, 2009).

128         Our primary interest is in the relationship between the centrality of a metabolite in the  
129 network and the sensitivity of that metabolite to mutation. Roughly speaking, the centrality of a  
130 node in a network quantifies some measure of the importance of the node in the network  
131 (Koschützki and Schreiber, 2008). A generic property of empirical networks, including  
132 metabolic networks, is that they are (approximately) scale-free; scale-free networks are  
133 characterized by a topology with a few "hub" nodes (high centrality) and many peripheral nodes  
134 (low centrality; Jeong et al., 2000). Scale-free networks are more robust to random perturbation  
135 than are randomly-connected networks (Albert et al., 2000).

136         Mutation is an important source of perturbation to biological systems, and much effort  
137 has gone into theoretical and empirical characterization of the conditions under which mutational

138 robustness will evolve (Wagner et al., 1997; de Visser et al., 2003; Proulx et al., 2007).  
139 Mutational robustness can be assessed in two basic ways: top-down, in which a known element  
140 of the system is mutated and the downstream effects of the mutation quantified, or bottom-up, in  
141 which mutations are introduced at random, either spontaneously or by mutagenesis, and the  
142 downstream effects quantified. Top-down experiments are straightforward to interpret: the  
143 greater the effects of the mutation (e.g., on a phenotype of interest), the less robust the system.  
144 However, the scope of inference is limited to the types of mutations introduced by the  
145 investigator (which in practice are almost always gene knockouts), and provide limited insight  
146 into natural variation in mutational robustness.

147 Bottom-up approaches, in which mutations are allowed to accumulate at random, provide  
148 insight into the evolution of a system as it actually exists in nature: all else equal, a system, or  
149 element of a system ("trait"), that is robust to the effects of mutation will accumulate less genetic  
150 variance under MA conditions than one that is not robust (Figure 1b; Stearns et al., 1995).  
151 However, the inference is not straightforward, because all else may not be equal: different  
152 systems or traits may present different mutational targets (roughly speaking, the number of sites  
153 in the genome that potentially affect a trait; Houle (1998)).

154 Ultimately, disentangling the evolutionary relationship between network architecture,  
155 mutational robustness, and mutational target is an empirical enterprise, specific to the system of  
156 interest. As a first step, it is necessary to establish the relationship between network architecture  
157 (e.g., topology) and the rate of accumulation of genetic variance under MA conditions. If a  
158 general relationship emerges, targeted top-down experiments can then be employed to dissect the  
159 relationship in more mechanistic detail.



160 In addition to the relationship between metabolite centrality and mutational variance, we  
161 are also interested in the relationship between network topology and the mutational correlation  
162 ( $r_M$ ) between pairs of metabolites (Figure 1c). In principle, mutational correlations reflect  
163 pleiotropic relationships between genes underlying pairs of traits (but see below for caveats;  
164 Estes et al., 2005). Genetic networks are often modular (Newman, 2006), consisting of groups of  
165 genes (modules) within which pleiotropy is strong and between which pleiotropy is weak  
166 (Wagner et al., 2007). Genetic modularity implies that mutational correlations will be negatively  
167 correlated with the length of the shortest path between network elements. However, it is possible  
168 that the network of gene interactions underlying metabolic regulation is not tightly correlated  
169 with the metabolic network itself, e.g., if *trans* acting regulation predominates.

170 Here we report results from a long-term MA experiment in the nematode *Caenorhabditis*  
171 *elegans*, in which replicate MA lines derived from a genetically homogeneous common ancestor  
172 (G0) were allowed to evolve under minimally effective selection ( $N_e \approx 1$ ) for approximately 250  
173 generations (Figure 1a). We previously reported estimates from these MA lines of two key  
174 quantitative genetic parameters by which the cumulative effects of mutation can be quantified:  
175 the per-generation change in the trait mean (the mutational bias,  $\Delta M$ ) and the per-generation  
176 increase in genetic variation (the mutational variance,  $V_M$ ) for the standing pools of 29  
177 metabolites (Davies et al., 2016); Supplementary Table S1. In this report, we interpret those  
178 results, and new estimates of mutational correlations ( $r_M$ ), in the context of the topology of the *C.*  
179 *elegans* metabolic network.

180

181 **Methods and Materials:**

182 I. Metabolic Network. The metabolic network of *C. elegans* was constructed following the  
183 criteria of Ma and Zeng (2003b), from two reaction databases (*i*) from Ma and Zeng (2003b);  
184 updated at <http://www.ibiodesign.net/kneva/>; we refer to this database as MZ, and (*ii*) from  
185 Yilmaz and Walhout (2016); <http://wormflux.umassmed.edu/>; we refer to this database as YW.  
186 Subnetworks that do not contain at least one of the 29 metabolites were excluded from  
187 downstream analyses. The method includes several *ad hoc* criteria for retaining or omitting  
188 specific metabolites from the analysis (criteria are listed on p. 272 of Ma and Zeng (2003b)).  
189 The set of reactions in the MZ and YW databases are approximately 99% congruent; in the few  
190 cases in which there is a discrepancy (listed in Supplementary Table S2), we chose to use the MZ  
191 database because we used the MZ criteria for categorizing currency metabolites (defined below).

192 To begin, the 29 metabolites of interest were identified and used as starting sites for the  
193 network. Next, all forward and reverse reactions stemming from the 29 metabolites were  
194 incorporated into the subnetwork until all reactions either looped back to the starting point or  
195 reached an endpoint. Currency metabolites were removed following the MZ criteria; a currency  
196 metabolite is roughly defined as a molecule such as water, proton, ATP, NADH, etc., that  
197 appears in a large fraction of metabolic reactions but is not itself an intermediate in an enzymatic  
198 pathway. Metabolic networks in which currency metabolites are included have much shorter  
199 paths than networks in which they are excluded. When currency metabolites are included in the  
200 network reported here, all shortest paths are reduced to no more than three steps, and most of the  
201 shortest paths consist of one or two steps. The biological relevance of path length when currency  
202 metabolites are included in the network is unclear (Ma and Zeng, 2003b).

203 A graphical representation of the network was constructed with the Pajek software  
204 package (<http://mrvar.fdv.uni-lj.si/pajek/>) and imported into the networkX Python package

205 (Hagberg et al., 2008). Proper importation from Pajek to networkX was verified by visual  
206 inspection.

207 II. Network Parameters. Properties of networks can be quantified in many ways, and different  
208 measures of network centrality capture different features of network importance (Table 1). We  
209 did not have strong prior hypotheses about which specific measure(s) of centrality associated  
210 with a given metabolite would prove most informative in terms of a relationship with the  
211 mutational properties of that metabolite (i.e.,  $\Delta M$  and/or  $V_M$ ). Therefore, we assessed the  
212 relationship between the mutational properties of a metabolite and several measures of its  
213 network centrality: betweenness, closeness, and degree centrality, in- and out-degree, and core  
214 number (depicted in Figure 3). These network parameters are all positively correlated.

215 Definitions of the parameters are given in Table 1; correlations between the parameters are  
216 included in Table 2. Calculation of network parameters was done using built-in functions in  
217 NetworkX.

218 III. Mutation Accumulation Lines. A full description of the construction and propagation of the  
219 mutation accumulation (MA) lines is given in Baer et al. (2005). Briefly, 100 replicate MA lines  
220 were initiated from a nearly-isogenic population of N2-strain *C. elegans* and propagated by  
221 single-hermaphrodite descent at four-day (one generation) intervals for approximately 250  
222 generations. The long-term  $N_e$  of the MA lines is very close to one, which means that mutations  
223 with a selective effect less than about 25% are effectively neutral (Keightley and Caballero,  
224 1997). The common ancestor of the MA lines ("G0") was cryopreserved at the outset of the  
225 experiment; MA lines were cryopreserved upon completion of the MA phase of the experiment.  
226 Based on extensive whole-genome sequencing (Denver et al., 2012; Saxena et al., submitted), we  
227 estimate that each MA line carries approximately 70 mutant alleles in the homozygous state.

228           At the time the metabolomics experiments reported in Davies et al. (2016) were initiated,  
229 approximately 70 of the 100 MA lines remained extant, of which 43 ultimately provided  
230 sufficient material for Gas Chromatography/Mass Spectrometry (GC-MS). Each MA line was  
231 initially replicated five-fold, although not all replicates provided data of sufficient quality to  
232 include in subsequent analyses; the mean number of replicates included per MA line is 3.9 (range  
233 = 2 to 5). The G0 ancestor was replicated nine times. However, the G0 ancestor was not  
234 subdivided into "pseudolines" (Teotónio et al., 2017), which means that inferences about  
235 mutational variances and covariances are necessarily predicated on the assumption that the  
236 among-line (co)variance of the ancestor is zero.

237           Each replicate consisted of stage-synchronized young adult worms taken from a single 10  
238 cm agar plate. Cultures were stage-synchronized by treatment with hypochlorite ("bleaching")  
239 following Stiernagle (2006); details of the synchronization are given in Davies et al. (2016).  
240 Following synchronization, worms were incubated at 20°C until young adulthood, defined as the  
241 point at which some eggs were seen on plates but no second generation worms had hatched. At  
242 this point, worms were washed from plates and collected for metabolomics. Each sample  
243 contained tens of thousands of worms, and although the samples were stage-synchronized, there  
244 was almost certainly some variation among samples in both the relative frequency of eggs on the  
245 plate and the (small) proportion of worms that had yet to reach adulthood.

246           Recently, whole-genome sequencing revealed that two MA lines, MA563 and MA564,  
247 share approximately 2/3 of their accumulated mutations; the simplest explanation is that the two  
248 lines were cross-contaminated around generation 150-175 of the MA protocol. However,  
249 averaged over all metabolites, the between-line standard deviation of those two lines is >3X that  
250 of either within-line SD, which suggests that the ~1/3 of the mutations in each genome that are

251 unique to each line contribute meaningfully to the differences between those two lines.  
252 Accordingly, we chose to include both lines. Further, since only 21 (out of 33) lines that we  
253 sequenced are represented in the metabolome dataset, the possibility of further unidentified  
254 cross-contamination cannot be ruled out. Comparisons between metabolites will not be biased  
255 by shared mutations, although the sampling (co)variance will increase by a factor  $k \leq \frac{N}{N-x+1}$ ,  
256 where  $N$  is the total number of lines and  $x$  is the number of lines that share mutations;  $k = \frac{N}{N-x+1}$   
257 if all lines that share mutations share all their mutations.

258 IV. Metabolomics. Details of the extraction and quantification of metabolites are given in  
259 Davies et al. (2016). Briefly, samples were analyzed using an Agilent 5975c quadrupole mass  
260 spectrometer with a 7890 gas chromatograph. Metabolites were identified by comparison of  
261 GC-MS features to the Fiehn Library (Kind et al., 2009) using the AMDIS deconvolution  
262 software (Halket et al., 1999), followed by reintegration of peaks using the GAVIN Matlab script  
263 (Behrends et al., 2011). Metabolites were quantified and normalized relative to an external  
264 quantitation standard. 34 metabolites were identified, of which 29 were ultimately included in  
265 the analyses. Normalized metabolite data are archived in Dryad  
266 (<http://dx.doi.org/10.5061/dryad.2dn09>).

267 V. Mutational Parameters. In what follows, a "trait" is the (normalized) concentration of a  
268 metabolite. There are three mutational parameters of interest: (i) the per-generation proportional  
269 change in the trait mean, referred to as the mutational bias,  $\Delta M$ ; (ii) the per-generation increase  
270 in the genetic variance, referred to as the mutational variance,  $V_M$ ; and (iii) the genetic  
271 correlation between the cumulative effects of mutations affecting pairs of traits, the mutational  
272 correlation,  $r_M$ . Details of the calculations of  $\Delta M$  and  $V_M$  are reported in Davies et al. (2016); we  
273 reprise the basic calculations here.

274 (i) *Mutational bias ( $\Delta M$ )* – The mutational bias is the change in the trait mean due to the  
275 cumulative effects of all mutations accrued over one generation.  $\Delta M_z = \mu_G \alpha_z$ , where  $\mu_G$  is the per-  
276 genome mutation rate and  $\alpha_z$  is the average effect of a mutation on trait  $z$ , and is calculated as  
277  $\Delta M_z = \frac{\bar{z}_{MA} - \bar{z}_0}{t \bar{z}_0}$ , where  $\bar{z}_{MA}$  and  $\bar{z}_0$  represent the MA and ancestral (G0) trait means and  $t$  is the  
278 number of generations of MA. However, the  $\Delta M$  was not normally distributed among the 29  
279 metabolites, so for downstream analyses we transformed  $\Delta M$  as  $\Delta M^* = \log_2\left(\frac{MA}{G0}\right)$ , where MA and  
280 G0 represent the trait values of the MA lines and the G0 ancestor, respectively;  $\Delta M = 2^{\Delta M^*} - 1$ .  
281 (ii) *Mutational variance ( $V_M$ )* - The mutational variance is the increase in the genetic variance  
282 due to the cumulative effects of all mutations accrued over one generation.  $V_M = \mu_G \alpha_z^2$  and is  
283 calculated as  $V_M = \Delta V_L = \frac{V_{L,MA} - V_{L,G0}}{2t}$ , where  $V_{L,MA}$  is the variance among MA lines,  $V_{L,G0}$  is the  
284 among-line variance in the G0 ancestor, and  $t$  is the number of generations of MA (Lynch and  
285 Walsh, 1998, p. 330). In this study, we must assume that  $V_{L,G0} = 0$ .

286 Comparisons of variation among traits or groups require that the variance be measured on  
287 a common scale.  $V_M$  is commonly scaled either relative to the trait mean, in which case  $V_M$  is  
288 the squared coefficient of variation and is often designated  $I_M$ , or relative to the residual variance,  
289  $V_E$ ;  $V_M/V_E$  is the mutational heritability,  $h_M^2$ .  $I_M$  and  $h_M^2$  have different statistical properties and  
290 evolutionary interpretations (Houle et al., 1996), so we report both. For each metabolite,  $I_M$  and  
291  $I_E$  are standardized relative to the mean of the MA lines. Both  $h_M^2$  and  $I_M$  were natural-log  
292 transformed to meet assumptions of normality prior to downstream analyses.

293 (iii) *Mutational correlation,  $r_M$*  – Pairwise mutational correlations were calculated from the  
294 among-line components of (co)variance, which were estimated by REML as implemented in the  
295 in the MIXED procedure of SAS v. 9.4, following Fry (2004). Statistical significance of

296 individual correlations was assessed by Z-test, with a global 5% significance criterion of  
297 approximately  $P < 0.000167$ .

298 VI. Analysis of the relationship between mutational parameters and network centrality. The six  
299 network parameters are all positively correlated, as are the four mutational parameters (Table 2).  
300 To assess the overall correlation structure between mutational and network parameters, we  
301 employed a hierarchical canonical correlation analysis (CCA), as implemented in the  
302 CANCORR procedure of SAS v. 9.4, with the network parameters as the "X" variables and the  
303 mutational parameters as the "Y" variables. We initially included all four mutational parameters,  
304 resulting in four pairs of canonical variates and four canonical correlations. We then repeated  
305 the analysis for each mutational parameter  $Y_i$  individually with the full set of six network  
306 parameters, resulting in one pair of canonical variates and one canonical correlation for each of  
307 the four mutational parameters. Finally, we calculated the pairwise correlation between all  
308 mutational parameters and all network parameters. For all analyses except the first, significance  
309 was assessed using the False Discovery Rate (FDR) (Benjamini and Hochberg, 1995).

310 IIV. Analysis of the relationship between mutational correlation ( $r_M$ ) and network architecture.

311 *(i) Correlation between mutational correlation ( $r_M$ ) and shortest path length.* Statistical  
312 assessment of the correlation between mutational correlation ( $r_M$ ) and shortest path length  
313 presents a problem of non-independence, for two reasons. First, all correlations including the  
314 same variable (metabolite) are non-independent; each of the  $n$  elements of an  $n \times n$  correlation  
315 matrix contributes to  $n(n-1)/2$  correlations. Second, even though the mutational correlation  
316 between metabolites  $i$  and  $j$  is the same as the mutational correlation between  $j$  and  $i$ , the shortest  
317 path lengths need not be the same, and moreover, the path from  $i$  to  $j$  may exist whereas the path  
318 from  $j$  to  $i$  may not (depicted in Supplementary Figure S1). To account for non-independence of

319 the data, we devised a parametric bootstrap procedure. Three metabolites (L-tryptophan, L-  
320 lysine, and Pantothenate) lie outside of the great strong component of the network (Ma and Zeng,  
321 2003a) and are omitted from the analysis. Each off-diagonal element of the 24x24 mutational  
322 correlation matrix ( $r_{ij}=r_{ji}$ ) was associated with a random shortest path length sampled with  
323 probability equal to its frequency in the empirical distribution of shortest path lengths between  
324 all metabolites included in the analysis. Next, we calculated the Spearman's correlation  $\rho$   
325 between  $r_M$  and the shortest path length. The procedure was repeated 10,000 times to generate  
326 an empirical distribution of  $\rho$ , to which the observed  $\rho$  can be compared. This comparison was  
327 done for the raw mutational correlation,  $r_M$ , the absolute value,  $|r_M|$ , and between  $r_M$  and the  
328 shortest path length in the undirected network (i.e., the shorter of the two paths between  
329 metabolites  $i$  and  $j$ ).

330

## 331 **Results and Discussion**

332 Representation of the Metabolic Network – The metabolic network of *C. elegans* was estimated  
333 using method of Ma and Zeng (2003b) from two independent but largely congruent databases  
334 (Ma and Zeng, 2003b; Yilmaz and Walhout, 2016). Details of the network construction are given  
335 in section I of the Methods; data are presented in Supplementary Appendix A1. For the set of  
336 metabolites included (see Methods), networks constructed from the MZ and YW databases give  
337 nearly identical results. In the few cases in which there is a discrepancy (~1%; Supplementary  
338 Table S2), we use the MZ network, for reasons we explain in the Methods. The resulting  
339 network is a directed graph including 646 metabolites, with 1203 reactions connecting nearly all  
340 metabolites (Figure 2).



341 Network centrality and sensitivity to mutation – Canonical correlation analysis did not identify  
342 significant correlation between mutational parameters and network parameters, either  
343 collectively (Figure 4; Supplementary Table S3) or individually. Further, of the 24 pairwise  
344 correlations between mutational parameters and network parameters (Table 2, Supplementary  
345 Figure S2), only the correlation between mutational heritability ( $h_M^2$ ) and core number  
346 approaches statistical significance ( $r=0.53$ , FDR < 0.1).

347 On the face of it, it appears there is no association between network centrality and any  
348 measure of mutational sensitivity. If so, there are various possible explanations. For example, it  
349 may be that mutational target and mutational robustness effectively cancel each other out. More  
350 worryingly, it may be that the representation of the *C. elegans* metabolic network used here  
351 misrepresents the network as it actually exists *in vivo*. For example, the topology of the dynamic  
352 metabolic network of the bacterium *E. coli* varies depending on the environmental context  
353 (Koschützki et al., 2010), and it seems intuitive that the greater spatiotemporal complexity  
354 inherent to a multicellular organism would exacerbate that problem. Or, most straightforwardly,  
355 it may be that there simply is no functional relationship between the centrality of a metabolite in  
356 a network and its sensitivity to mutation.

357 However, several trends apparent in the results suggest the conservative interpretation  
358 may miss meaningful signal emerging from noisy data. First, the point estimates of the  
359 canonical correlations are not small (> 0.45 in all five cases; e.g., the first canonical correlation  
360 in the full analysis is 0.69; Supplementary Table 3); it may simply be that the sampling variance  
361 associated with the relatively small number of mutations, MA lines and (especially) metabolites  
362 overwhelms the signal of a weak but consistently positive association. Second, of the 24  
363 pairwise correlations among mutational and network parameters (Table 2), only five are

364 negative, significantly fewer than expected at random if the variables are uncorrelated  
365 (cumulative binomial probability = 0.0033). Third, the point estimates of the pairwise  
366 correlations are not random with respect to either network or mutational parameters. For all four  
367 mutational parameters, the correlation is greatest with core number (exact probability  $\approx$   
368 0.00077). Core number is a discrete interval variable, whereas the other measures of network  
369 centrality are continuous variables. Quantifying centrality in terms of core number is analogous  
370 to categorizing a set of size measurements into "small" and "large": power is increased, at the  
371 cost of losing the ability to discriminate between subtler differences.

372 Fourth, for five out of six network parameters, the correlation is greatest with  $h_M^2$  (exact  
373 cumulative probability  $\approx$  0.00066).  $V_M$  is the numerator of both  $h_M^2$  and  $I_M$ ; the difference is the  
374 denominator, with  $h_M^2$  scaling  $V_M$  by the residual variance,  $V_E$ , and  $I_M$  scaling  $V_M$  by the square  
375 of the trait mean. If  $V_E$  was more strongly associated with network topology than was  $V_M$ ,  $h_M^2$   
376 would presumably be more strongly correlated with network parameters than would  $I_M$ ,  
377 analogous to the well-documented  $V_E$ -driven negative association between the narrow-sense  
378 heritability of a trait and the correlation of the trait with fitness (Houle, 1992). However,  $I_M$  and  
379  $I_E$  are nearly identically (un)correlated with network parameters (Table 2), so that scenario  
380 cannot explain the correlation. Coincidence seems as likely an explanation as any.

381 The relationship between mutational correlation ( $r_M$ ) and shortest path length – In an MA  
382 experiment, the cumulative effects of mutations on a pair of traits  $i$  and  $j$  may covary for two,  
383 nonexclusive reasons (Estes et al., 2005). More interestingly, individual mutations may have  
384 consistently pleiotropic effects, such that mutations that affect trait  $i$  also affect trait  $j$  in a  
385 consistent way. Less interestingly, but unavoidably, individual MA lines will have accumulated  
386 different numbers of mutations, and if mutations have consistently directional effects, as would

387 be expected for traits correlated with fitness, lines with more mutations will have more extreme  
388 trait values than lines with fewer mutations, even in the absence of consistent pleiotropy. Estes  
389 et al. (2005) simulated the sampling process in *C. elegans* MA lines with mutational properties  
390 derived from empirical estimates from a variety of traits and concluded that sampling is not  
391 likely to lead to large absolute mutational correlations in the absence of consistent pleiotropy  
392 ( $|r_M| \leq 0.25$ ).

393 Ideally, we would like to estimate the full mutational (co)variance matrix,  $\mathbf{M}$ , from the  
394 joint estimate of the among-line (co)variance matrix. However, with 25 traits, there are  $(25 \times 26) / 2$   
395 = 325 covariances, and with only 43 MA lines, there is insufficient information to jointly  
396 estimate the restricted maximum likelihood of the full  $\mathbf{M}$  matrix. To proceed, we calculated  
397 mutational correlations from pairwise REML estimates of the among-line (co)variances, i.e.,  
398  $r_M = \frac{COV_L(X,Y)}{\sqrt{VAR_L(X)VAR_L(Y)}}$  (Clark et al., 1995; Mezey and Houle, 2005). Pairwise estimates of  $r_M$  are  
399 shown in Supplementary Table S4. To assess the extent to which the pairwise correlations are  
400 sensitive to the underlying covariance structure, we devised a heuristic bootstrap analysis. For a  
401 random subset of 12 of the 300 pairs of traits, we randomly sampled six of the remaining 23  
402 traits without replacement and estimated  $r_M$  between the two focal traits from the joint REML  
403 among-line (co)variance matrix. For each of the 12 pairs of focal traits, we repeated the analysis  
404 100 times.

405 There is a technical caveat to the preceding bootstrap analysis. Resampling statistics are  
406 predicated on the assumption that the variables are exchangeable (Shaw, 1992), which  
407 metabolites are not. For that reason, we do not present confidence intervals on the resampled  
408 correlations, only the distributions. However, we believe that the analysis provides a meaningful

409 heuristic by which the sensitivity of the pairwise correlations to the underlying covariance  
410 structure can be assessed.

411 Distributions of resampled correlations are shown in Supplementary Figure S3. In every  
412 case the point estimate of  $r_M$  falls on the mode of the distribution of resampled correlations, and  
413 in 11 of the 12 cases, the median of the resampled distribution is very close to the point estimate  
414 of  $r_M$ . However, in six of the 12 cases, some fraction of the resampled distribution falls outside  
415 two standard errors of the point estimate. The most important point that the resampling analysis  
416 reveals is this: given that 29 metabolites encompass only a small fraction of the total metabolome  
417 of *C. elegans* (<5%), even had we been able to estimate the joint likelihood of the full  $29 \times 30/2$   
418  $M$ -matrix, the true covariance relationships among those 29 metabolites could conceivably be  
419 quite different from those estimated from the data.

420 The simplest property that describes the relationship between two nodes in a network is  
421 the length of the shortest path between them (= number of edges). In a directed network, such as  
422 a metabolic network, the shortest path from element  $i$  to element  $j$  is not necessarily the same as  
423 the shortest path from  $j$  to  $i$ . For each pair of metabolites  $i$  and  $j$ , we calculated the shortest path  
424 length from  $i$  to  $j$  and from  $j$  to  $i$ , without repeated walks (Supplementary Table S5). We then  
425 calculated Spearman's correlation  $\rho$  between the mutational correlation  $r_M$  and the shortest path  
426 length.

427 There is a weak, but significant, negative correlation between  $r_M$  and the shortest path  
428 length between the two metabolites ( $\rho = -0.128$ , two-tailed  $P < 0.03$ ; Figure 5a), whereas  $|r_M|$  is  
429 not significantly correlated with shortest path length ( $\rho = -0.0058$ , two-tailed  $P > 0.45$ ;  
430 Supplementary Figure 5b). The correlation between  $r_M$  and the shortest path in the undirected

431 network is similar to the correlation between  $r_M$  and the shortest path in the directed network ( $\rho =$   
432  $-0.105$ , two-tailed  $P > 0.10$ ; Supplementary Figure 5c).

433 An intuitive possible cause of the weak negative association between shortest path length  
434 and mutational correlation would be if a mutation that perturbs a metabolic pathway toward the  
435 beginning of the pathway has effects that propagate downstream in the same pathway, but the  
436 effect of the perturbation attenuates. The attenuation could be due either to random noise or to  
437 the effects of other inputs into the pathway downstream from the perturbation (or both). The net  
438 effect would be a characteristic pathway length past which the mutational effects on two  
439 metabolites are uncorrelated, leading to an overall negative correlation between  $r_M$  and path  
440 length. The finding that the correlations between  $r_M$  and the shortest path length in the directed  
441 and undirected network are very similar reinforces that conclusion. The negative correlation  
442 between  $r_M$  and shortest path length is reminiscent of a finding from Arabidopsis, in which sets  
443 of metabolites significantly altered by single random gene knockouts are closer in the global  
444 metabolic network than expected by chance (Kim et al., 2015).

#### 445 Conclusions and Future Directions

446 The proximate goal of this study was to find out if there are topological properties of the *C.*  
447 *elegans* metabolic network (node centrality, shortest path length) that are correlated with a set of  
448 statistical descriptions of the cumulative effects of spontaneous mutations ( $\Delta M$ ,  $V_M$ ,  $r_M$ ).  
449 Ultimately, we hope that a deeper understanding of those mathematical relationships will shed  
450 light on the mechanistic biology of the organism. Bearing in mind the statistical fragility of the  
451 results, we conclude:

452 (i) Network centrality may be associated with mutational sensitivity ( $V_M$ ); it is not associated  
453 with mutational robustness ( $1/V_M$ ). If in fact the apparently non-random features of the data

454 represent a hint of signal emerging from the noise, the most plausible explanation is that  
455 metabolites that are central in the network present a larger mutational target than do metabolites  
456 that peripherally located. Somewhat analogously, Landry et al. (2007) investigated the  
457 mutational properties of transcription in a set of yeast MA lines and found that  $h_M^2$  is positively  
458 correlated with both the number of genes with which a given gene interacts ("trans-mutational  
459 target") and the number of transcription factor binding sites in a gene's promoter ("cis-mutational  
460 target"). Those authors did not formally quantify the network properties of the set of transcripts,  
461 although it seems likely that mutational target size as they defined it is positively correlated with  
462 centrality in the transcriptional network. It is important to note, however, although  $1/V_M$  is a  
463 meaningful measure of mutational robustness (Stearns and Kawecki, 1994), it does not  
464 necessarily follow that highly-connected metabolites are therefore more robust to the effects of  
465 *individual* mutations (Houle, 1998; Ho and Zhang, 2016).

466 *(ii) Pleiotropic effects of mutations affecting the metabolome are predominantly local, as*  
467 evidenced by the significant negative correlation between the mutational correlation,  $r_M$ , and the  
468 shortest path length between a pair of metabolites. That result is not surprising in hindsight, but  
469 the weakness of the correlation suggests that there are other important factors that underlie  
470 pleiotropy beyond network proximity.

471 *(iii) Future Directions.* To advance understanding of the mutability of the *C. elegans* metabolic  
472 network, three things are needed. First, it will be important to cover a larger fraction of the  
473 metabolic network. Untargeted mass spectrometry of cultures of *C. elegans* reveals many  
474 thousands of features (Art Edison, personal communication); 29 metabolites are only the tip of a  
475 large iceberg. For example, our intuition leads us to believe that the mutability of a metabolite  
476 will depend more on its in-degree (mathematically, the number of edges leading into a node in a

477 directed graph; biochemically, the number of reactions in which the metabolite is a product) than  
478 its out-degree. For all four mutational parameters, the point-estimate of the pairwise correlation  
479 with in-degree is greater than that with out-degree (Table 2), although that result is not  
480 statistically significant (binomial probability = 0.0625).

481         Second, to more precisely partition mutational (co)variance into within- and among-line  
482 components, more MA lines are needed. We estimate that each MA line carries about 70 unique  
483 mutations (see Methods), thus the mutational (co)variance is the result of about 3000 total  
484 mutations, distributed among 43 MA lines. The MA lines were a preexisting resource, and the  
485 sample size was predetermined. It is encouraging that we were able to detect significant  
486 mutational variance for 25/29 metabolites (Supplementary Table S1), but only 14% (42/300) of  
487 pairwise mutational correlations are significantly different from zero at the experiment-wide 5%  
488 significance level, roughly corresponding to  $|r_M| > 0.5$  (Supplementary Table S4); 18 of the 42  
489 significant mutational correlations are not significantly different from  $|r_M| = 1$ . It remains  
490 uncertain how sensitive estimates of mutational correlations are to the underlying covariance  
491 structure of the metabolome. It also remains to be seen if the mutability of specific features of  
492 metabolic networks are genotype or species-specific, and the extent to which mutability depends  
493 on environmental context.

494         Third, it will be important to quantify metabolites (static concentrations and fluxes) with  
495 more precision. The metabolite data analyzed in this study were collected from large cultures  
496 ( $n > 10,000$  individuals) of approximately stage-synchronized worms, and were normalized  
497 relative to an external quantitation standard (Davies et al., 2016). Ideally, one would like to  
498 characterize the metabolomes of single individuals, assayed at the identical stage of  
499 development. Single-worm metabolomics is on the near horizon (M. Witting, personal

500 communication). Minimizing the number of individuals in a sample is important for two  
501 reasons; (1) the smaller the sample, the easier it is to be certain the individuals are at the same  
502 developmental stage, and (2) knowing the exact number of individuals in a sample makes  
503 normalization relative to an external standard more interpretable. Ideally, data would be  
504 normalized relative to both an external standard and an internal standard (e.g., total protein;  
505 Clark et al. (1995)).

506 This study provides an initial assessment of the relationship between mutation and  
507 metabolic network architecture. To begin to uncover the relationship between metabolic  
508 architecture and natural selection, the next step is to repeat these analyses with respect to the  
509 standing genetic variation ( $V_G$ ). There is some reason to think that more centrally-positioned  
510 metabolites will be more evolutionarily constrained (i.e., under stronger purifying selection) than  
511 peripheral metabolites (Vitkup et al., 2006), in which case the ratio of the mutational variance to  
512 the standing genetic variance ( $V_M/V_G$ ) will increase with increasing centrality.

513

#### 514 **Acknowledgments** –

515 This work was initially conceived by Armand Leroi and Jake Bundy. We thank Art Edison, Dan  
516 Hahn, Tom Hladish, Marta Wayne, Michael Witting, and several anonymous reviewers for their  
517 generosity and helpful advice. We especially thank Hongwu Ma for leading us to and through his  
518 metabolite database and Reviewer #3 for his/her many insightful comments and suggestions.

519 Support was provided by NIH grant R01GM107227 to CFB and E. C. Andersen.

520



## 521 **References Cited**

- 522 Albert, R., Jeong, H., and Barabasi, A.L. (2000). Error and attack tolerance of complex networks. *Nature*  
523 406, 378-382.
- 524 Baer, C.F., Shaw, F., Steding, C., Baumgartner, M., Hawkins, A., Houppert, A., Mason, N., Reed, M.,  
525 Simonelic, K., Woodard, W., and Lynch, M. (2005). Comparative evolutionary genetics of  
526 spontaneous mutations affecting fitness in rhabditid nematodes. *Proceedings of the National*  
527 *Academy of Sciences of the United States of America* 102, 5785-5790.
- 528 Batagelj, V., and Zaversnik, M. (2011). Fast algorithms for determining (generalized) core groups in social  
529 networks. *Advances in Data Analysis and Classification* 5, 129-145.
- 530 Behrends, V., Tredwell, G.D., and Bundy, J.G. (2011). Gavin, a add-on to AMDIS, new GUI-driven version.  
531 *Analytical Biochemistry* 415 206–208.
- 532 Benjamini, Y., and Hochberg, Y. (1995). Controlling the false discovery rate - a practical and powerful  
533 approach to multiple testing. *Journal of the Royal Statistical Society Series B-Methodological* 57,  
534 289-300.
- 535 Bernhardsson, S., and Minnhagen, P. (2010). Selective pressure on metabolic network structures as  
536 measured from the random blind-watchmaker network. *New Journal of Physics* 12.
- 537 Clark, A.G., Wang, L., and Hulleberg, T. (1995). Spontaneous mutation rate of modifiers of metabolism in  
538 *Drosophila*. *Genetics* 139, 767-779.
- 539 Davies, S.K., Leroi, A.M., Burt, A., Bundy, J., and Baer, C.F. (2016). The mutational structure of  
540 metabolism in *Caenorhabditis elegans*. *Evolution* 70, 2239-2246.
- 541 De Visser, J., Hermisson, J., Wagner, G.P., Meyers, L.A., Bagheri, H.C., Blanchard, J.L., Chao, L., Cheverud,  
542 J.M., Elena, S.F., Fontana, W., Gibson, G., Hansen, T.F., Krakauer, D., Lewontin, R.C., Ofria, C.,  
543 Rice, S.H., Von Dassow, G., Wagner, A., and Whitlock, M.C. (2003). Perspective: Evolution and  
544 detection of genetic robustness. *Evolution* 57, 1959-1972.
- 545 Denver, D.R., Wilhelm, L.J., Howe, D.K., Gafner, K., Dolan, P.C., and Baer, C.F. (2012). Variation in base-  
546 substitution mutation in experimental and natural lineages of *Caenorhabditis* nematodes.  
547 *Genome Biology and Evolution* 4, 513-522.
- 548 Estes, S., Ajie, B.C., Lynch, M., and Phillips, P.C. (2005). Spontaneous mutational correlations for life-  
549 history, morphological and behavioral characters in *Caenorhabditis elegans*. *Genetics* 170, 645-  
550 653.
- 551 Fell, D.A., and Wagner, A. (2000). The small world of metabolism. *Nature Biotechnology* 18, 1121-1122.
- 552 Fry, J.D. (2004). "Estimation of genetic variances and covariances by restricted maximum likelihood using  
553 PROC MIXED," in *Genetic Analysis of Complex Traits Using SAS*, ed. A.M. Saxton. (Cary, NC: SAS  
554 Institute, Inc.), 11-34.
- 555 Greenberg, A.J., Stockwell, S.R., and Clark, A.G. (2008). Evolutionary Constraint and Adaptation in the  
556 Metabolic Network of *Drosophila*. *Molecular Biology and Evolution* 25, 2537-2546.
- 557 Hagberg, A.A., Schult, D.A., and Swart, P.J. (Year). "Exploring network structure, dynamics, and function  
558 using NetworkX", in: *7th Python in Science Conference (SciPy2008)*, eds. G. Varoquaux, T. Vaught  
559 & J. Millman).
- 560 Halket, J.M., Przyborowska, A., Stein, S.E., Mallard, W.G., Down, S., and Chalmers, R.A. (1999).  
561 Deconvolution gas chromatography/mass spectrometry of urinary organic acids -- potential for  
562 pattern recognition and automated identification of metabolic disorders. *Rapid Communications*  
563 *in Mass Spectrometry* 13, 279-284.
- 564 Halligan, D.L., and Keightley, P.D. (2009). Spontaneous mutation accumulation studies in evolutionary  
565 genetics. *Annual Review of Ecology Evolution and Systematics* 40, 151-172.
- 566 Ho, W.C., and Zhang, J.Z. (2016). Adaptive Genetic Robustness of *Escherichia coli* Metabolic Fluxes.  
567 *Molecular Biology and Evolution* 33, 1164-1176.

- 568 Houle, D. (1992). Comparing evolvability and variability of quantitative traits. *Genetics* 130, 195-204.
- 569 Houle, D. (1998). How should we explain variation in the genetic variance of traits? *Genetica* 103, 241-  
570 253.
- 571 Houle, D., Morikawa, B., and Lynch, M. (1996). Comparing mutational variabilities. *Genetics* 143, 1467-  
572 1483.
- 573 Hudson, C.M., and Conant, G.C. (2011). Expression level, cellular compartment and metabolic network  
574 position all influence the average selective constraint on mammalian enzymes. *Bmc Evolutionary*  
575 *Biology* 11.
- 576 Jeong, H., Tombor, B., Albert, R., Oltvai, Z.N., and Barabasi, A.L. (2000). The large-scale organization of  
577 metabolic networks. *Nature* 407, 651-654.
- 578 Keightley, P.D., and Caballero, A. (1997). Genomic mutation rates for lifetime reproductive output and  
579 lifespan in *Caenorhabditis elegans*. *Proceedings of the National Academy of Sciences of the*  
580 *United States of America* 94, 3823-3827.
- 581 Kim, T., Dreher, K., Nilo-Poyanco, R., Lee, I., Fiehn, O., Lange, B.M., Nikolau, B.J., Sumner, L., Welti, R.,  
582 Wurtele, E.S., and Rhee, S.Y. (2015). Patterns of Metabolite Changes Identified from Large-Scale  
583 Gene Perturbations in Arabidopsis Using a Genome-Scale Metabolic Network. *Plant Physiology*  
584 167, 1685-U1890.
- 585 Kimura, M. (1968). Evolutionary rate at the molecular level. *Nature* 217, 624-626.
- 586 Kind, T., Wohlgemuth, G., Lee Do, Y., Lu, Y., Palazoglu, M., S, S., and Fiehn, O. (2009 ). Mass spectral and  
587 retention index libraries for metabolomics based on quadrupole and time-of-flight gas  
588 chromatography/mass spectrometry. *Analytical Chemistry* 81, 10038-10048.
- 589 Koschützki, D., Junker, B.H., Schwender, J., and Schreiber, F. (2010). Structural analysis of metabolic  
590 networks based on flux centrality. *Journal of Theoretical Biology* 265, 261-269.
- 591 Koschützki, D., and Schreiber, F. (2008). Centrality analysis methods for biological networks and their  
592 application to gene regulatory networks. *Gene Regulation and Systems Biology* 2008, 193-201.
- 593 Landry, C.R., Lemos, B., Rifkin, S.A., Dickinson, W.J., and Hartl, D.L. (2007). Genetic properties influencing  
594 the evolvability of gene expression. *Science* 317, 118-121.
- 595 Levy, S.F., and Siegal, M.L. (2008). Network hubs buffer environmental variation in *Saccharomyces*  
596 *cerevisiae*. *PLoS Biology* 6, 2588-2604.
- 597 Lynch, M., and Walsh, B. (1998). *Genetics and Analysis of Quantitative Traits*. Sunderland, MA.: Sinauer.
- 598 Ma, H.W., and Zeng, A.P. (2003a). The connectivity structure, giant strong component and centrality of  
599 metabolic networks. *Bioinformatics* 19, 1423-1430.
- 600 Ma, H.W., and Zeng, A.P. (2003b). Reconstruction of metabolic networks from genome data and analysis  
601 of their global structure for various organisms. *Bioinformatics* 19, 270-277.
- 602 Mezey, J.G., and Houle, D. (2005). The dimensionality of genetic variation for wing shape in *Drosophila*  
603 *melanogaster*. *Evolution* 59, 1027-1038.
- 604 Minnhagen, P., and Bernhardsson, S. (2008). The Blind Watchmaker Network: Scale-Freeness and  
605 Evolution. *PLoS One* 3.
- 606 Newman, M.E.J. (2006). Modularity and community structure in networks. *Proceedings of the National*  
607 *Academy of Sciences of the United States of America* 103, 8577-8582.
- 608 Papp, B., Teusink, B., and Notabaart, R.A. (2009). A critical view of metabolic network adaptations. *Hfsp*  
609 *Journal* 3, 24-35.
- 610 Proulx, S.R., Nuzhdin, S.V., and Promislow, D.E.L. (2007). Direct selection on genetic robustness revealed  
611 in the yeast transcriptome. *PLoS One* 2, e911.
- 612 Shaw, R.G. (1992). Comparison of quantitative genetic parameters - reply. *Evolution* 46, 1967-1969.
- 613 Siegal, M.L., Promislow, D.E.L., and Bergman, A. (2007). Functional and evolutionary inference in gene  
614 networks: does topology matter? *Genetica* 129, 83-103.

- 615 Stearns, S.C., Kaiser, M., and Kawecki, T.J. (1995). The differential genetic and environmental  
616 canalization of fitness components in *Drosophila melanogaster*. *Journal of Evolutionary Biology*  
617 8, 539-557.
- 618 Stearns, S.C., and Kawecki, T.J. (1994). Fitness sensitivity and the canalization of life-history traits.  
619 *Evolution* 48, 1438-1450.
- 620 Stiernagle, T. (2006). "Maintenance of *C. elegans*", in: *WormBook*. (ed.) T.C.E.R. Community.).
- 621 Teotónio, H., Estes, S., Phillips, P.C., and Baer, C.F. (2017). Experimental Evolution with *Caenorhabditis*  
622 *Nematodes*. *Genetics* 206, 691-716.
- 623 Vitkup, D., Kharchenko, P., and Wagner, A. (2006). Influence of metabolic network structure and  
624 function on enzyme evolution. *Genome Biology* 7.
- 625 Wagner, A., and Fell, D.A. (2001). The small world inside large metabolic networks. *Proceedings of the*  
626 *Royal Society B-Biological Sciences* 268, 1803-1810.
- 627 Wagner, G.P., Booth, G., and Bagheri, H.C. (1997). A population genetic theory of canalization. *Evolution*  
628 51, 329-347.
- 629 Wagner, G.P., Pavlicev, M., and Cheverud, J.M. (2007). The road to modularity. *Nature Reviews Genetics*  
630 8, 921-931.
- 631 Winterbach, W., Van Mieghem, P., Reinders, M., Wang, H.J., and De Ridder, D. (2013). Topology of  
632 molecular interaction networks. *Bmc Systems Biology* 7.
- 633 Yilmaz, L.S., and Walhout, Albertha j.M. (2016). A *Caenorhabditis elegans* genome-scale metabolic  
634 network model. *Cell Systems* 2, 297-311.

635

636

## Figure Legends

**Figure 1.** (a) Schematic diagram of the mutation accumulation (MA) experiment. An MA experiment is simply a pedigree. The genetically homogeneous ancestral line (G0) was subdivided into 100 MA lines, of which 43 are included in this study. Lines were allowed to accumulate mutations for  $t=250$  generations. At each generation, lines were propagated by a single randomly chosen hermaphrodite ( $N=1$ ). Mutations, represented as colored blocks within a homologous pair of chromosomes, arise initially as heterozygotes and are either lost or fixed over the course of the experiment. At the culmination of the experiment, each line has accumulated its own unique set of mutations. MA lines were compared to the cryopreserved G0 ancestor, which is wild-type at all loci. After Halligan and Keightley (2009). (b) Expected outcome of an MA experiment. As mutations accumulate over time, relative fitness (solid dark blue line) declines from its initial value of 1 at rate  $\Delta M$  per generation and the genetic component of variance (solid orange line) increases from its initial value of 0 at rate  $V_M$  per generation. Trait X (light blue dashed line) is positively correlated with fitness and declines with MA; trait Y (green dashed line) is negatively correlated with fitness and increases with MA. Trajectories are depicted as linear, but they need not be. (c) Accumulation of mutational covariance in an MA experiment. Coordinate axes represent two traits, X and Y. Concentric ellipses show the increase in genetic covariance with MA, beginning from the initial value of zero; the orientation of the ellipses (red arrow) represents the linear relationship between pleiotropic mutational effects on the two traits.

**Figure 2.** Graphical depiction of the metabolic network including all 29 metabolites. Pink nodes represent included metabolites with core number = 1, red nodes represent included metabolites with core number = 2. Gray nodes represent metabolites with which the included 29 metabolites directly interact. Metabolite identification numbers are: 1, L-Serine; 2, Glycine; 3, Nicotinate; 4, Succinate; 5, Uracil; 6, Fumarate; 7, L-Methionine; 8, L-Alanine. 9, L-Aspartate; 10, L-3-Amino-isobutanoate; 11, trans-4-Hydroxy-L-proline; 12, (S) – Malate; 13, 5-Oxoproline; 14, L-Glutamate; 15, L-Phenylalanine; 16, L-Asparagine; 17, D-Ribose; 18, Putrescine; 19, Citrate; 20, Adenine; 21, L-Lysine; 22, L-Tyrosine; 23, Pantothenate; 24, Xanthine; 25, Hexadecanoic acid; 26, Urate; 27, L-Tryptophan; 28, Adenosine; 29, Alpha;alpha-Trehalose.

**Figure 3.** Schematic depiction of the  $k$ -cores of a graph. The  $k$ -core of a graph is the largest subgraph that contains nodes of degree at least  $k$ . The colored balls represent nodes in a network and the black lines represent connecting edges. Each dark red ball in the white area has core number  $k=3$ ; note that each node with  $k=3$  is connected to at least three other nodes. The depicted graph is undirected. After Batagelj and Zaversnik (2011).

**Figure 4.** Plot of first canonical variate pair; the network variate is plotted on the X-axis, the mutation variate is plotted on the Y-axis. Each data point represents a metabolite; the numbers are the metabolite identifiers given in the legend to Figure 2. Metabolites with core number = 1 are in pink, metabolites with core number = 2 are in red.

**Figure 5.** Parametric bootstrap distributions of random correlations  $\rho$  between (a)  $r_M$  and the shortest path length in the directed network, (b)  $|r_M|$  and the shortest path length in the directed

network, (c)  $r_M$  and shortest path length in the undirected network (i.e., the shorter of the two path lengths between metabolites  $i$  and  $j$  in the directed network). Orange lines show the observed values of  $\rho$ , black lines show the 95% confidence interval of the distribution of the correlation between the mutational correlation and a random shortest path length drawn from the observed distribution of shortest path lengths. See Methods for details.

In review

Parameter	Heuristic Definition	Formal Definition
In Degree ( <b>IN</b> <sup>o</sup> ), $deg^+(v)$	The number of incoming edges to node $v$ in a directed graph.	self-explanatory
Out Degree ( <b>OUT</b> <sup>o</sup> ), $deg^-(v)$	The number of outgoing edges from node $v$ in a directed graph.	self-explanatory
Shortest Path Length, $d(v, u)$	Shortest distance from node $v$ to another node $u$ with no repeated walks	self-explanatory
Betweenness Centrality ( <b>BET</b> ), $c_B(v)$	Betweenness centrality of node $v$ is the sum of the fraction of all-pairs shortest paths that pass through $v$ . The greater $c_B(v)$ , the greater the fraction of shortest paths that pass through node $v$ .	$\frac{c_B(v)}{(n-1)(n-2)}$ , where $c_B(v) = \sum_{s,t \in V} \frac{\sigma(s,t v)}{\sigma(s,t)}$ , $V$ is the set of nodes, $\sigma(s, t)$ is the number of shortest paths from node $s$ to node $t$ , $\sigma(s, t v)$ is the number of paths from $s$ to $t$ that pass through node $v$ , and $n$ is the number of nodes in the graph. The denominator $(n-1)(n-2)$ is the normalization factor for a directed graph that scales $c_B(v)$ between 0 and 1.

Parameter	Heuristic Definition	Formal Definition
Closeness Centrality ( <b>CLO</b> ), $C(v)$	Closeness centrality of node $v$ is the reciprocal of the sum of the shortest path lengths to all $n-1$ other nodes, normalized by the sum of minimum possible distances $n-1$ . The greater $C(v)$ , the closer $v$ is to other nodes.	$C(v) = \frac{n-1}{\sum_{u=1}^{n-1} d(u,v)}$ , where $n$ is the number of nodes and $d(u, v)$ is the shortest path distance between $u$ and $v$ .
Degree Centrality ( <b>DEG</b> ), $C_D(v)$	Degree centrality of node $v$ is the fraction of nodes in the network that node $v$ is connected to.	$C_D(v) = \frac{deg^+(v)+deg^-(v)}{n-1}$ , where $n$ is the number of nodes in the network.
Core Number ( <b>CORE</b> )	A $k$ -core is the largest subgraph that contains nodes of at least degree $k$ . The core number of node $v$ is the largest value $k$ of a $k$ -core containing node $v$ .	Calculated using the algorithm of Batagelj and Zaversnik (2011).
Mutational Bias ( <b>ΔM</b> )	Per-generation rate of change of the trait mean in an MA experiment. Equivalent to the product of the genome-wide mutation rate, $\mu_G$ , and the average effect of a mutation on the trait, $\alpha$ .	$\Delta M_z = \frac{\bar{z}_{MA} - \bar{z}_0}{t\bar{z}_0}$ ; $\bar{z}_{MA}$ and $\bar{z}_0$ represent the MA and ancestral (G0) trait means and $t$ is the number of generations of MA.



Parameter	Heuristic Definition	Formal Definition
Mutational Variance ( $V_M$ )	Per-generation rate of increase in genetic variance for a trait in an MA experiment. Equivalent to the product of the genome-wide mutation rate, $\mu_G$ , and the square of the average effect of a mutation on the trait, $\alpha^2$ .	$V_M = \Delta V_L = \frac{V_{L,MA} - V_{L,G0}}{2t}$ , where $V_{L,MA}$ is the variance among MA lines, $V_{L,G0}$ is the among-line variance in the G0 ancestor, and $t$ is the number of generations of MA
Squared coefficient of variation ( $I_M, I_E$ )	$I_M$ is the mutational variance ( $V_M$ ) scaled by the square of the trait mean, and provides a measure of the evolvability of a trait. $I_E$ is the residual variance ( $V_E$ ) scaled in the same way.	
Mutational heritability ( $h_M^2$ )	Mutational variance ( $V_M$ ) scaled as a fraction of the residual variance ( $V_E$ ). Provides a measure of the short-term response to selection on mutational variance.	$h_M^2 = \frac{V_M}{V_E}$

<b>Parameter</b>	<b>Heuristic Definition</b>	<b>Formal Definition</b>
Mutational correlation ( <b><math>r_M</math></b> )	Genetic correlation between two traits in MA lines. Provides an estimate of pleiotropic effects of new mutations.	$r_M = \frac{COV_M(X,Y)}{\sqrt{V_M(X)V_M(Y)}}$ , where $COV_M$ is the mutational covariance and $V_M$ is the mutational variance.

**Table 1.** Definitions of network parameters, following the documentation of NetworkX, v.1.11 (Hagberg et al. 2008) and mutational parameters. Abbreviations of the parameters used in Table 2 follow the parameter name in parentheses in bold type.

	<b>BTW</b>	<b>CLO</b>	<b>DEG</b>	<b>IN<sup>o</sup></b>	<b>OUT<sup>o</sup></b>	<b>CORE</b>	<b>ΔM</b>	<b> ΔM </b>	<b><math>h_M^2</math></b>	<b><math>I_M</math></b>	<b><math>I_E</math></b>
<b>BTW</b>		0.43	0.49	0.52	0.39	0.48	-0.16	-0.14	0.03	-0.06	-0.10
<b>CLO</b>			0.52	0.51	0.45	0.52	0.14	0.21	0.21	0.27	0.06
<b>DEG</b>				0.90	0.93	0.79	0.09	0.06	0.25	0.15	0.16
<b>IN<sup>o</sup></b>					0.67	0.82	0.22	0.23	0.30	0.21	0.25
<b>OUT<sup>o</sup></b>						0.64	-0.04	-0.08	0.17	0.09	0.05
<b>CORE</b>							0.33	0.28	0.53*	0.30	0.28
<b>ΔM</b>								0.84	0.62	0.71	0.81
<b> ΔM </b>									0.53	0.69	0.84
<b><math>h_M^2</math></b>										0.72	0.43
<b><math>I_M</math></b>											0.82
<b><math>I_E</math></b>											

**Table 2.** Correlations between network parameters (Row/Column 1-5), between mutational parameters (Row/Column 6-9), between network and mutational parameters (shaded cells), and between residual variance ( $I_E$ , Row/Column 10) and network and mutational parameters.

Abbreviations of network parameters are: BTW, betweenness centrality; CLO, closeness centrality; DEG, degree centrality; IN<sup>o</sup>, in-degree, OUT<sup>o</sup>, out-degree; CORE, core number.

Abbreviations of mutational parameters are: ΔM, per-generation change in the trait mean; |ΔM|, absolute value of ΔM;  $h_M^2$ , mutational heritability;  $I_M$ , squared mutational CV;  $I_E$ , squared residual CV. Network and mutational parameters are defined in Table 1. See text and Supplementary Table S1 for details of mutational parameters.\* FDR < 0.1

Figure 1.TIF

bioRxiv preprint first posted online Aug. 28, 2017; doi: <http://dx.doi.org/10.1101/181511>. The copyright holder for this preprint (which was not peer-reviewed) is the author/funder, who has granted bioRxiv a license to display the preprint in perpetuity. It is made available under a [CC-BY-NC-ND 4.0 International license](https://creativecommons.org/licenses/by-nc-nd/4.0/).

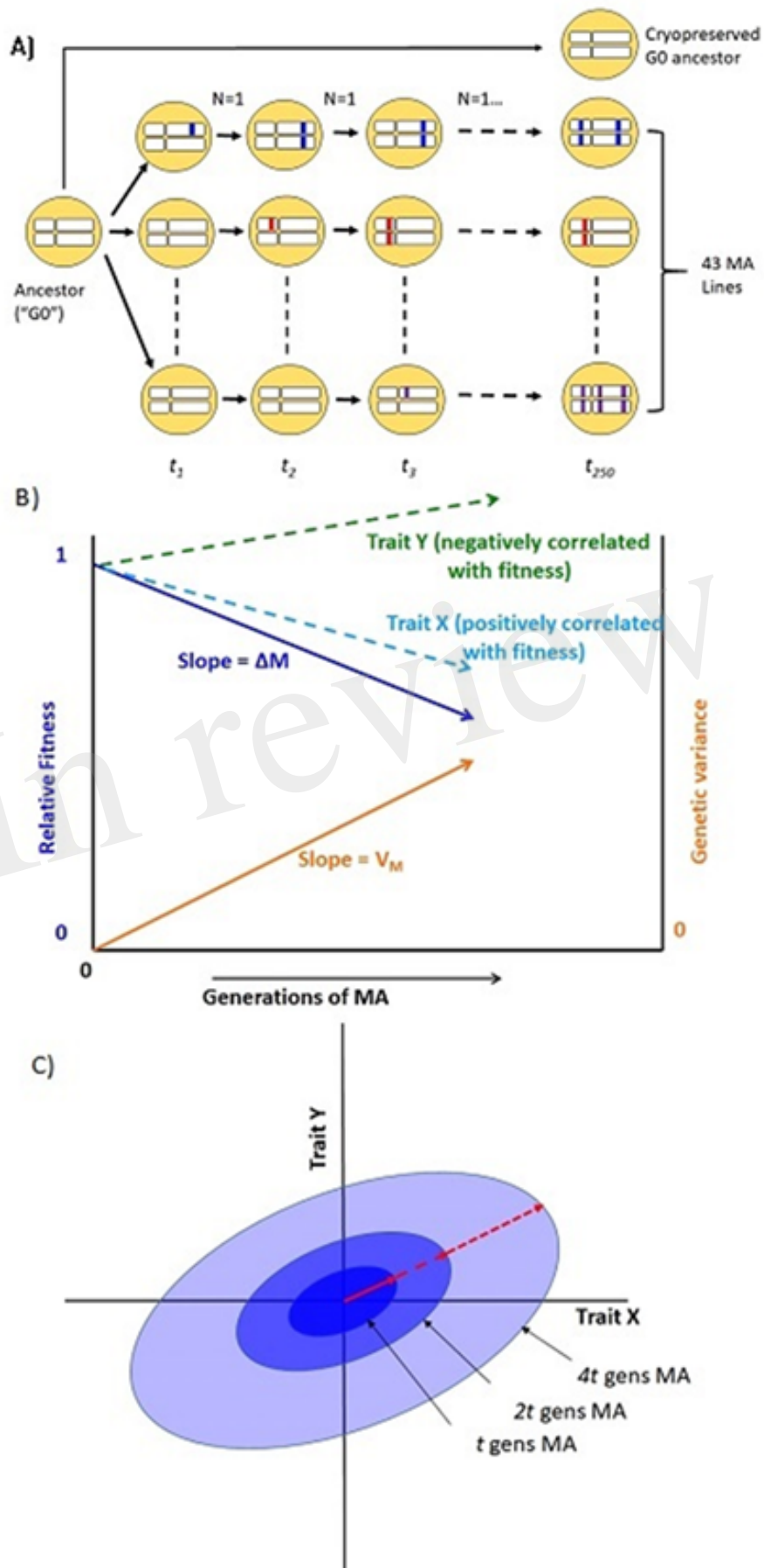


Figure 2.TIF

bioRxiv preprint first posted online Aug. 28, 2017; doi: <http://dx.doi.org/10.1101/181511>. The copyright holder for this preprint (which was not peer-reviewed) is the author/funder, who has granted bioRxiv a license to display the preprint in perpetuity. It is made available under a [CC-BY-NC-ND 4.0 International license](https://creativecommons.org/licenses/by-nc-nd/4.0/).

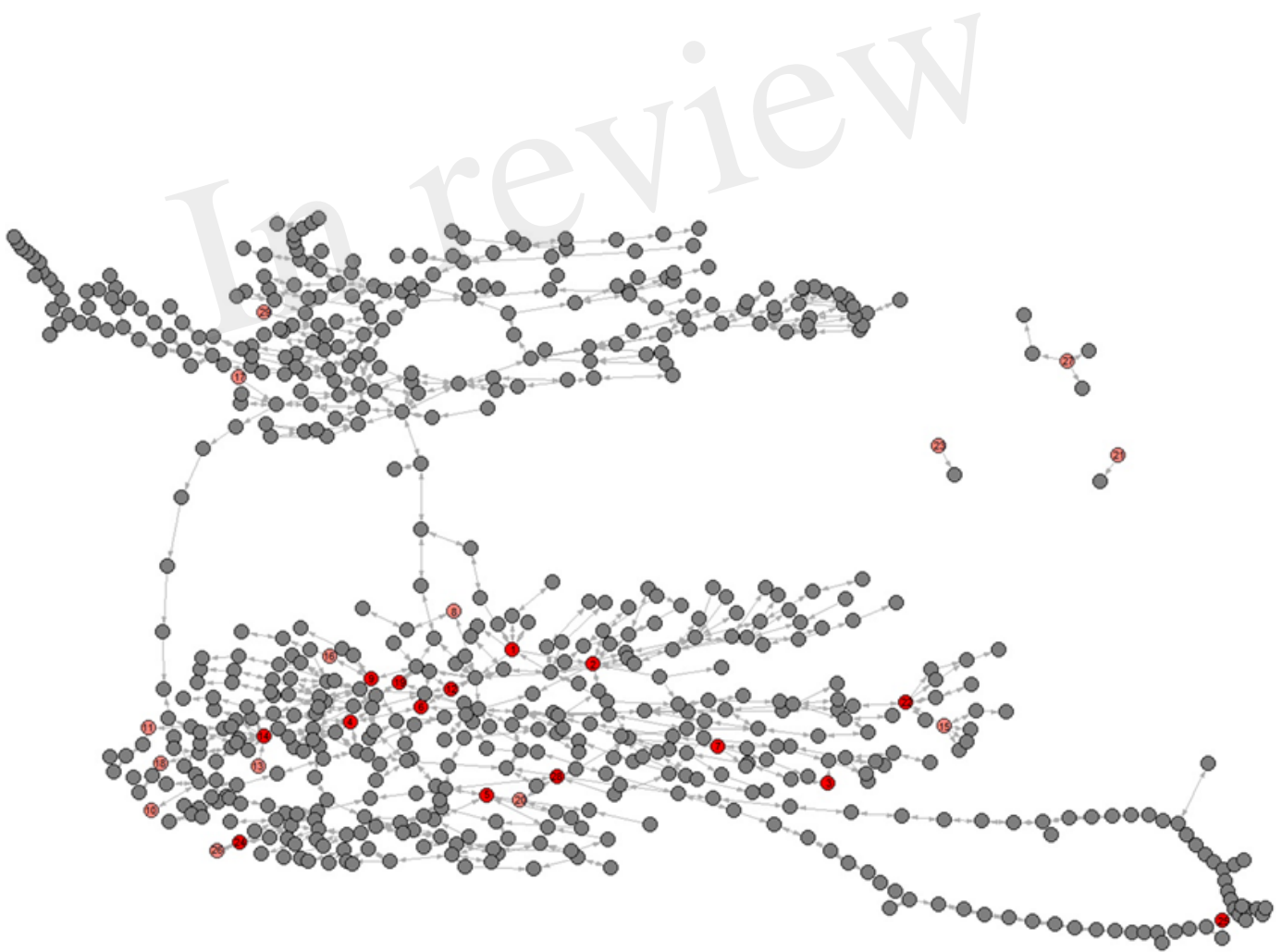


Figure 3.TIF

bioRxiv preprint first posted online Aug. 28, 2017; doi: <http://dx.doi.org/10.1101/181511>. The copyright holder for this preprint (which was not peer-reviewed) is the author/funder, who has granted bioRxiv a license to display the preprint in perpetuity. It is made available under a [CC-BY-NC-ND 4.0 International license](https://creativecommons.org/licenses/by-nc-nd/4.0/).

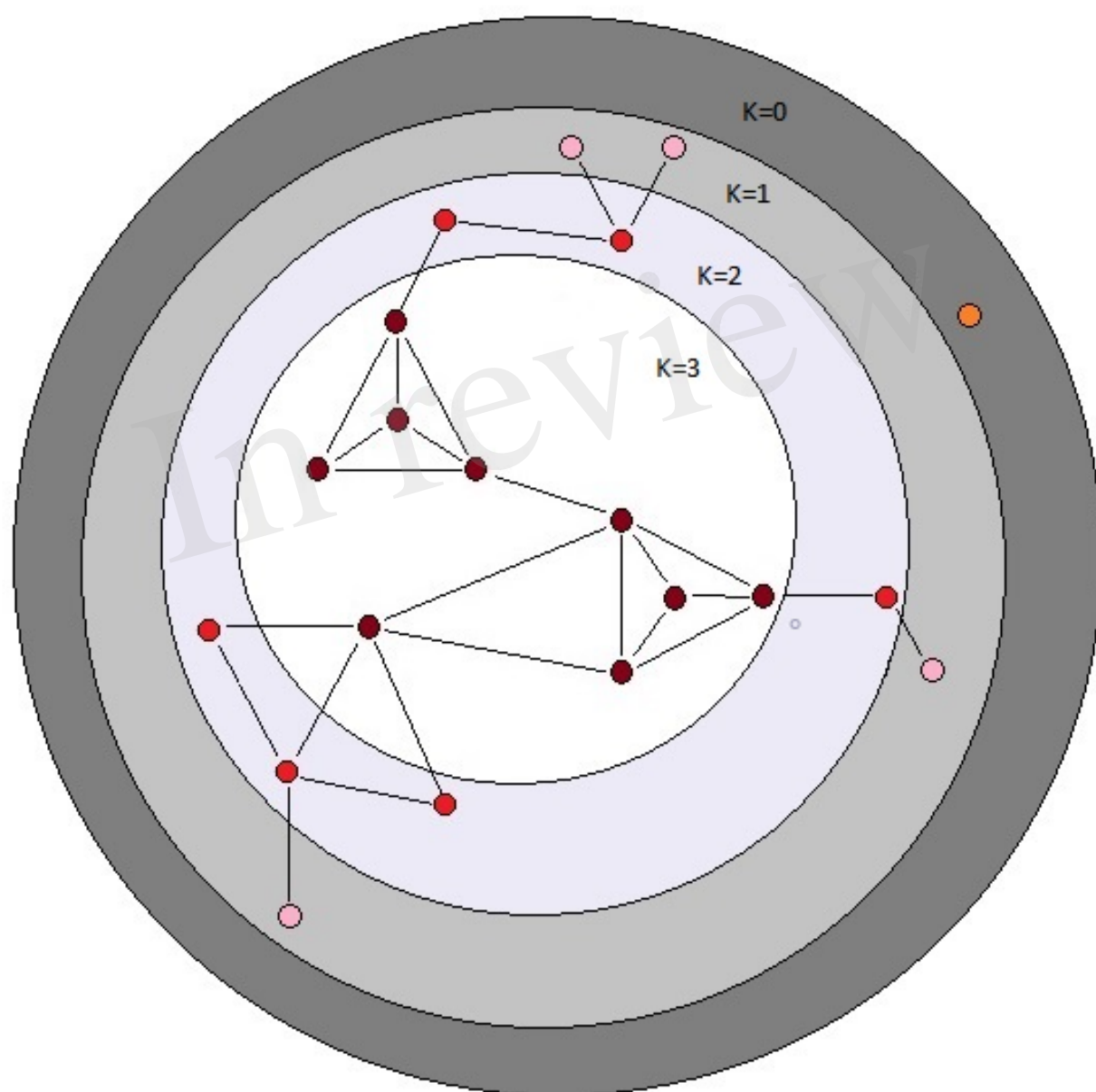


Figure 4.TIF

bioRxiv preprint first posted online Aug. 28, 2017; doi: <http://dx.doi.org/10.1101/181511>. The copyright holder for this preprint (which was not peer-reviewed) is the author/funder, who has granted bioRxiv a license to display the preprint in perpetuity. It is made available under a [CC-BY-NC-ND 4.0 International license](https://creativecommons.org/licenses/by-nc-nd/4.0/).

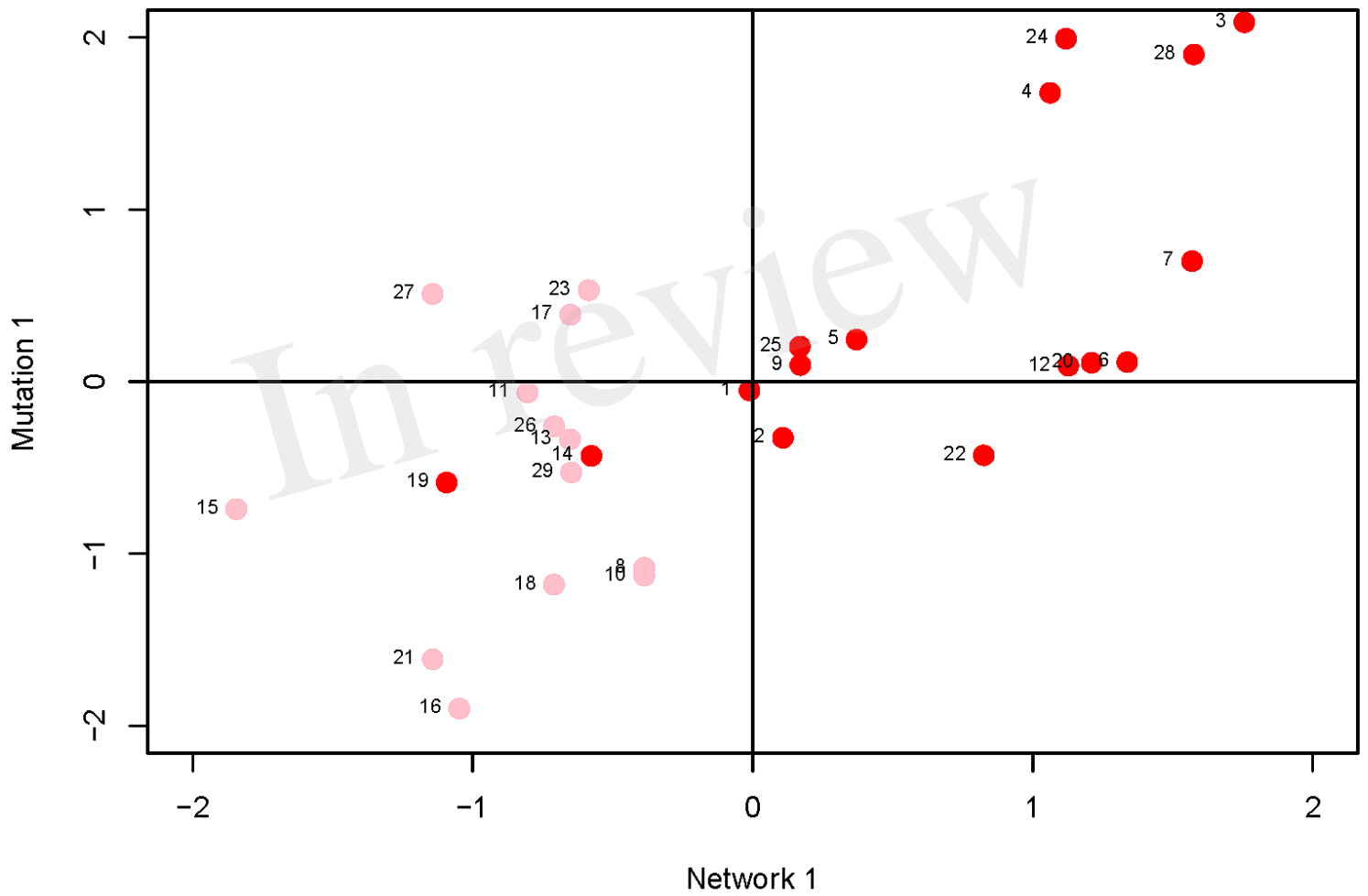


Figure 5.TIF

bioRxiv preprint first posted online Aug. 28, 2017; doi: <http://dx.doi.org/10.1101/181511>. The copyright holder for this preprint (which was not peer-reviewed) is the author/funder, who has granted bioRxiv a license to display the preprint in perpetuity. It is made available under a [CC-BY-NC-ND 4.0 International license](https://creativecommons.org/licenses/by-nc-nd/4.0/).

